FACETS AND FACET SUBGRAPHS OF ADJACENCY POLYTOPES

TIANRAN CHEN[1], ROBERT DAVIS[2], AND EVGENIIA KORCHEVSKAIA[1,3]

Abstract. Adjacency polytopes, a.k.a. symmetric edge polytopes, associated with undirected graphs have been defined and studied in several seemingly-independent areas including number theory, discrete geometry, and dynamical systems. In particular, the authors are motivated by the study of the algebraic Kuramoto equations of unmixed form whose Newton polytopes are the adjacency polytopes.

The interplay between the geometric structure of adjacency polytopes and the topological structure of the underlying graphs is a recurring theme in recent studies. In particular, "facet/face subgraphs" emerged as one of the central concepts in describing this symmetry. Continuing along this line of inquiry we provide a complete description of the correspondence between facets/faces of an adjacency polytope and maximal bipartite subgraphs of the underlying connected graph.

1. Introduction

For a connected graph G with nodes $\mathcal{V}(G) = \{0, 1, \ldots, n\}$ and edge set $\mathcal{E}(G)$, its *adjacency polytope* [4] (a.k.a. *symmetric edge polytope* [16]) is the convex polytope $\operatorname{conv}\{\mathbf{e}_i - \mathbf{e}_j \mid \{i, j\} \in \mathcal{E}(G)\}$ where $\mathbf{e}_0 = \mathbf{0}$ and $\mathbf{e}_i$ is the i^{th} standard basis vector. In the context of Kuramoto models [15], the geometric structure of adjacency polytopes has been instrumental in solving the root counting problem for algebraic Kuramoto equations [5, 6, 15]. In the broader context, the adjacency polytope of G is equivalent to the symmetric edge polytope, which has been studied by number theorists, combinatorialists, and discrete geometers motivated by several seemingly-independent problems [11, 12, 13, 16, 17, 18, 19]. These different viewpoints are consolidated in recent work by D'Alì, Delucchi, and Michałek [10] which, among other contributions, sheds new light on the structure of adjacency polytopes of bipartite graphs, cycles, wheels, and graphs consisting of two subgraphs sharing a single edge. Using Gröbner basis methods, the authors provide explicit formulae for the number of facets and the normalized volume of adjacency polytopes associated with several classes of graphs.

One recurring theme in these recent works is the symmetry between the geometric structure of adjacency polytopes and topological structure of the underlying graphs. In particular,

[1]Department of Mathematics, Auburn University Montgomery, Montgomery, AL, USA
[2]Department of Mathematics, Colgate University, Hamilton, NY, USA
[3](Current affiliation) School of Mathematics, Georgia Institute of Technology, Atlanta, GA, USA
E-mail addresses: ti@nranchen.org, rdavis@colgate.edu, ekorchev@gatech.edu.

1991 *Mathematics Subject Classification.* Primary 52B20, 52B40; Secondary 34C15.
Key words and phrases. Adjacency polytope, symmetric edge polytope, Kuramoto equations.
TC and RD are supported by the National Science Foundation under grants no. 1923099 and no. 1922998 respectively. TC and EK are supported by a grant from the Auburn University Montgomery Research Grant-in-Aid Program. EK is also supported by the Undergraduate Research Experience program funded by the Department of Mathematics at Auburn University at Montgomery .

the concept of "facet/face subgraphs" is defined and studied [3, 10]. The present work is a continuation along this line of research. The main contributions of this paper include the following descriptions of the correspondence between faces of an adjacency polytope and face subgraphs of the underlying graph.

- Facet subgraphs of a connected graph are exactly its maximal bipartite subgraphs. (Theorem 3 part (2))
- Connected face subgraphs of a connected graph are exactly its maximal bipartite subgraphs in their corresponding induced subgraphs. (Theorem 3 part (1))
- A complete description of the equivalence class of facets corresponding to a given facet of the adjacency polytope. (Theorem 9)
- Equivalence of geometric properties of faces and topological properties of the corresponding face subgraphs. (Theorem 12)

This paper is structured as follows. Section 2 states necessary definitions and notation. Section 3 reviews the construction of adjacency polytopes and face subgraphs. Section 4.1 provides a brief overview of existing results on the interplay between facets/faces of adjacency polytopes and their corresponding subgraphs. Then, in Section 4.2, we develop the main results. Section 4.3 highlights the important implications of the results in the study of algebraic Kuramoto equations. In Section 5, we illustrate how these results apply to a concrete class of non-bipartite graphs.

2. Preliminaries and notation

For a (undirected) graph G, let $\mathcal{V}(G)$ and $\mathcal{E}(G)$ denote its sets of vertices (i.e. nodes) and edges respectively. We use $\{i, j\}$ to denote the (undirected) edge connecting i and j. A simple graph is *bipartite* if it contains no odd cycles, i.e., it is 2-colorable. Ordering the set of bipartite subgraphs of a simple connected graph G by inclusion provides a partial ordering of these subgraphs. We call the maximal elements *maximal bipartite subgraphs* of G, and they are necessarily connected and spanning. For a subset $V \subseteq \mathcal{V}(G)$, the induced subgraph $G[V]$ is the subgraph consisting of all edges $\{i, j\} \in \mathcal{E}(G)$ where both $i, j \in V$. More generally, we use the notation $H < G$ to indicate H is a subgraph of G.

For a digraph $\vec{G}$, the arrowhead notation is used to emphasize the distinction between $\vec{G}$ and its underlying undirected graph G. A directed edge from i to j is denoted (i, j), and we use the notation $-(i, j) = (j, i)$. Similarly, the *transpose* of $\vec{G}$, which reverses the orientation of all edges in $\vec{G}$, is denoted $-\vec{G}$.

A (convex) *polytope* P in $\mathbb{R}^n$ is the convex hull of a finite set of points, that is,

$$P = \operatorname{conv}\{\mathbf{x}_1, \dots, \mathbf{x}_m\} = \left\{ \sum_{i=1}^{m} \lambda_i \mathbf{x}_i \mid \lambda_1, \dots, \lambda_m \geq 0, \sum_{i=1}^{m} \lambda_i = 1 \right\}$$

for some $\mathbf{x}_1, \dots, \mathbf{x}_m \in \mathbb{R}^n$. The *dimension* of P, denoted $\dim(P)$, is the dimension of the affine span of P. A nonempty *face* of P is a subset of P for which a linear functional $\langle \cdot, \boldsymbol{\alpha} \rangle$ is minimized. In this case, $\boldsymbol{\alpha}$ is an *inner normal* of the face. The empty set is also a face of P, called the *empty face*. Faces are themselves polytopes, where 0-dimensional faces are *vertices* and maximal proper faces of P are *facets*. The set of all facets of P is denoted by $\mathcal{F}(P)$. For a detailed treatment of polytopes in general, see e.g. [21].

In our discussion, we are mainly interested in the set of vertices from which a convex polytope is built. It is therefore convenient to focus on *point configurations* which are simply finite collections of labeled points. For a point configuration $X = \{\mathbf{x}_1, \dots, \mathbf{x}_m\}$, its dimension is defined by $\dim(X) = \dim(\operatorname{conv}(X))$. Similarly, $X' \subseteq X$ is a face (resp. facet) of X if $\operatorname{conv}(X')$ is a face (resp. facet) of $\operatorname{conv}(X)$. We say X is (affinely) *dependent* if there are real numbers $\lambda_1, \dots, \lambda_m$ with $\sum_{i=1}^m \lambda_i = 0$ such that $\sum_{i=1}^m \lambda_i \mathbf{x}_i = \mathbf{0}$. Otherwise, it is *independent*. Call X a *simplex* if $|X| = \dim(X) + 1$ and a *circuit* if it is dependent yet all of its proper subsets are independent. Its *corank* is the number $|X| - \dim(X) - 1$.

3. Adjacency polytopes

For a connected graph G with nodes $\mathcal{V}(G) = \{1, \dots, N\}$, its *adjacency polytope of PV-type* [4] is the convex polytope $\operatorname{conv}\{\pm(\mathbf{e}_{i-1} - \mathbf{e}_{j-1}) \mid \{i,j\} \in \mathcal{E}(G)\} \subset \mathbb{R}^n$, where $n = N-1$, $\mathbf{e}_i \in \mathbb{R}^n$ is the vector with 1 in the i-th entry and zero elsewhere, and $\mathbf{e}_0 = \mathbf{0}$. This is equivalent to the *symmetric edge polytope* [10, 16]. This family of polytopes is closely related to but is different from the adjacency polytopes of *PQ-type* [4, 8], whence the name "adjacency polytope" was derived. Since this paper only studies the adjacency polytopes of PV-type, they will simply be referred to as *adjacency polytopes.* Moreover, since we are mostly interested in combinatorial aspects of adjacency polytopes, it is more convenient to focus on the underlying finite point configuration. We define

$$\check{\nabla}_G = \{\pm(\mathbf{e}_{i-1} - \mathbf{e}_{j-1}) \mid \{i,j\} \in \mathcal{E}(G)\} \subset \mathbb{R}^n = \mathbb{R}^{N-1}$$
$$\bar{\nabla}_G = \{\pm(\mathbf{e}_i - \mathbf{e}_j \mid \{i,j\}) \in \mathcal{E}(G)\} \subset \mathbb{R}^N.$$

These two point configurations have the same intrinsic geometric properties, and they only differ in the ambient space in which they are embedded: $\check{\nabla}_G$ is a full-dimensional point configuration in $\mathbb{R}^{N-1}$ whereas $\bar{\nabla}_G$ is a codimension-1 point configuration in $\mathbb{R}^N$, and $\check{\nabla}_G$ is precisely the projection of $\bar{\nabla}_G$ onto the last $N-1$ coordinates. The check mark notation in $\check{\nabla}_G$ is a reminder that it is a projection to a lower-dimensional subspace. We also extend this notation to their subsets, e.g., we identify any subset $X \subseteq \bar{\nabla}_G$ with its projection $\check{X} \subseteq \check{\nabla}_G$. When describing subsets of $\check{\nabla}_G$ or $\bar{\nabla}_G$, the "codimension" of a subset always refers to the codimension relative to $\check{\nabla}_G$ or $\bar{\nabla}_G$ themselves, regardless of the ambient space.

The projection that maps $\bar{\nabla}_G$ to $\check{\nabla}_G$ is a unimodular equivalence between the two configurations, and we will use both in our discussions. When referencing intrinsic geometric properties, the distinction between the two will not be relevant, and we will simply use ∇_G.

We also extend this construction to digraphs: for a digraph $\vec{G}$, we define

$$\check{\nabla}_{\vec{G}} = \{\mathbf{e}_{i-1} - \mathbf{e}_{j-1} \mid (i,j) \in \mathcal{E}(\vec{G})\} \subset \mathbb{R}^{N-1}$$
$$\bar{\nabla}_{\vec{G}} = \{\mathbf{e}_i - \mathbf{e}_j \mid (i,j) \in \mathcal{E}(\vec{G})\} \subset \mathbb{R}^N.$$

Here, $\mathbf{e}_i - \mathbf{e}_j \in \bar{\nabla}_{\vec{G}}$ no longer implies $\mathbf{e}_j - \mathbf{e}_i \in \bar{\nabla}_{\vec{G}}$, thus $\operatorname{conv}(\bar{\nabla}_{\vec{G}})$ may not be a symmetric edge polytope. The notations $\check{\nabla}_G, \bar{\nabla}_G$ and $\check{\nabla}_{\vec{G}}, \bar{\nabla}_{\vec{G}}$ extend naturally to subgraphs of G and directed subgraphs of a digraph $\vec{G}$, respectively, by restriction.

By construction, $\mathbf{0}$ is always an interior point of $\operatorname{conv}(\check{\nabla}_G)$, which allows the inner normals to be normalized to a certain form. We state this observation as a lemma for later reference.

Lemma 1. *For a connected nontrivial graph G, a nonzero vector $\check{\boldsymbol{\alpha}} \in \mathbb{R}^n$ is an inner normal of a d-dimensional face of $\check{\nabla}_G$ if and only if there are $\mathbf{x}_1, \dots, \mathbf{x}_{d+1} \in \check{\nabla}_G$ such that*

$\mathbf{x}_1, \ldots, \mathbf{x}_{d+1}$ *are linearly independent as vectors and*

$$\langle \mathbf{x}_i \,,\, c\check{\boldsymbol{\alpha}} \rangle = -1 \quad \textit{for any } i = 1, \ldots, d+1, \textit{and}$$
$$\langle \mathbf{x} \,,\, c\check{\boldsymbol{\alpha}} \rangle \geq -1 \quad \textit{for any } \mathbf{x} \in \check{\nabla}_G$$

for some positive real number c.

Inner normals that satisfy the above system will be referred to as **normalized inner normals**. Among them the vectors in $\mathbb{Z}^n$ having coprime coordinates are known as **primitive inner normals**. Of course, the same extends to inner normals for faces of $\bar{\nabla}_G$ since each inner normal of $\bar{\nabla}_G$ projects down to an inner normal of $\check{\nabla}_G$, and each inner normal of $\check{\nabla}_G$ lifts to an equivalence class of inner normals of $\bar{\nabla}_G$.

The central theme of this paper is the interplay between combinatorial properties of faces of ∇_G and graph-theoretic properties of subgraphs of G.

Definition 2. Given a connected graph G and a nonempty subset $X \subseteq \bar{\nabla}_G$, we define $\vec{G}_X$ and G_X to be the subgraphs with vertex and edge sets

$$\begin{aligned}
\mathcal{V}(\vec{G}_X) &= \{ i \mid \mathbf{e}_i - \mathbf{e}_j \in X \text{ or } \mathbf{e}_j - \mathbf{e}_i \in X \text{ for some } j \} \\
\mathcal{E}(\vec{G}_X) &= \{ \ (i,j) \ \mid \ \mathbf{e}_i - \mathbf{e}_j \in X \} \\
\mathcal{V}(G_X) &= \{ i \mid \mathbf{e}_i - \mathbf{e}_j \in X \text{ or } \mathbf{e}_j - \mathbf{e}_i \in X \text{ for some } j \} \\
\mathcal{E}(G_X) &= \{ \ \{i,j\} \ \mid \ \mathbf{e}_i - \mathbf{e}_j \in X \text{ or } \mathbf{e}_j - \mathbf{e}_i \in X \},
\end{aligned}$$

respectively. If F is a face (resp. facet) of ∇_G, then $\vec{G}_F$ is the **directed face (resp. facet) subgraph** associated with F, and G_F is the associated **face (resp. facet) subgraph**.

These concepts are defined and studied closely in recent works [3, 10]. The notations are the mirror images of the map $\vec{G} \mapsto \nabla_{\vec{G}}$, and the two interact in an expected way — for any subset X of ∇_G, we have $\nabla_{\vec{G}_X} = X$, and for any directed subgraph $\vec{H}$ of $\vec{G}$, we have $\vec{G}_{\nabla_{\vec{H}}} = \vec{H}$. The same holds for their directed counterparts.

In the above definition, points in X are exactly the columns in the incidence matrix of $\vec{G}_X$, which will be denoted by $Q(\vec{G}_X)$. The **truncated incidence** matrix $\check{Q}(\vec{G}_X)$, obtained by removing the first row of $Q(\vec{G}_X)$, corresponds to points in the projection $\check{X} \subset \check{\nabla}_G$.

4. Facets, faces, and associated subgraphs

In general, the collection of facets and their properties encode important geometric information about a convex polytope. The facets of an adjacency polytope $\operatorname{conv}(\nabla_G)$, in particular, have been closely studied from several different viewpoints [10]. We continue this line of inquiry through a graph-theoretical approach.

Recall that a face (resp. facet) subgraph (Definition 2) of G is a subgraph H for which there is a face (resp. facet) F of ∇_G such that $H = G_F$. Such facet subgraphs have been studied in connection to homotopy methods for solving algebraic Kuramoto equations [3]. In the broader context, facet subgraphs and face subgraphs were also classified algebraically [10, 12]. In Section 4.1, we briefly review of recent results on the interplay between facets/faces and their corresponding subgraphs. Then, in Section 4.2, we develop the main results. In particular, we aim to we provide a complete description of facet/face subgraphs as well as the equivalence classes of directed facet subgraphs. Important implications of these results in algebraic Kuramoto equations are highlighted in Section 4.3.

4.1. **Recent results on facets and facet subgraphs.** The role of facets of ∇_G as building blocks in the study of algebraic Kuramoto systems has been explored recently from the viewpoint of homotopy continuation methods [3]. Facets of ∇_G associated with even cycles are described from the viewpoint of Ehrhart theory by Ohsugi and Shibata [18]. Explicit descriptions of the facets of ∇_G, for G being trees and cycles are also established [6].

Using Gröbner basis methods, recent work of D'Alì, Delucchi, and Michałek [10] provides a broader and more detailed combinatorial description for the faces of ∇_G. In particular, the authors have shown that unimodular simplices contained in a facet $F \in \mathcal{F}(\nabla_G)$ correspond exactly to spanning trees of G_F [10, Corollary 3.3]. They also show that for a connected bipartite graph G, the total number of facets is bounded by $2^{|\mathcal{V}(G)|-1}$. In Section 4.2, we provide graph-theoretic refinements for both of these results.

For the adjacency polytope $\nabla_{C_{2k}}$ induced by an even cycle C_{2k}, the numbers of faces of all dimensions, i.e., the f-vector, are also computed [10, Proposition 4.3]. Moreover, if G_1 and G_2 are both connected bipartite graphs, and G is formed by joining G_1 and G_2 along an edge, it has been shown that $|\mathcal{F}(\nabla_G)| = \frac{1}{2} f_1 f_2$ where $f_1 = |\mathcal{F}(\nabla_{G_1})|$ and $f_2 = |\mathcal{F}(\nabla_{G_2})|$ [10, Proposition 4.10]. This result can be applied recursively and extended to graphs formed by joining multiple even cycles consecutively by an edge [10, Corollary 4.11].

4.2. **Main results.** Throughout this section, we take G to be a nontrivial, connected, and simple graph. Our goal is to clarify the structure of the map $F \mapsto G_F$ between facets/faces of ∇_G and subgraphs of G as well as how geometric and graph-theoretic properties are translated under this map.

Theorem 3 shows that connected face/facet subgraphs associated with faces/facets of ∇_G are exactly the maximal bipartite subgraphs of induced subgraphs of G. Corollary 4 generalizes this description to components of face subgraphs. In particular, the map $F \mapsto G_F$ is a surjective map from $\mathcal{F}(\nabla_G)$ to the set of maximal bipartite subgraphs of G. This map is not injective. Corollary 5 shows a canonical pair of choices for preimages for a given maximal bipartite subgraph under this map, and Remark 6 provides the graph-theoretic interpretation: These canonical choices of facets corresponding to a maximal bipartite subgraph are given by cut-sets with uniform orientation.

In general, permutations of the signs of points in a given facet F may produce other facets of ∇_G corresponding to the same maximal bipartite subgraph. Theorem 7 describes necessary balancing conditions imposed on such permutations by cycles in G. Conversely, Theorem 8 provides sufficient conditions for a subset of ∇_G to be a facet. Extending on these results, Theorem 9 states an explicit parametrization of the equivalence class of facets corresponding to the same facet subgraph in terms of fundamental cycles. From this parametrization, we derive generalizations, in Corollaries 10 and 11, to the upper bound of the total number of facets ∇_G has from recent works [6, 10]. In Theorem 12, we explore the connection between geometric properties of subsets of facets and the topological properties of their corresponding subgraphs through the lens of matroid theory. Using these properties, we derive the equivalence that an adjacency polytope will be simplicial if and only if the corresponding connected graph contains no even cycles (Corollary 14).

Theorem 3. *Let G be a connected graph.*

(1) *A connected nontrivial subgraph H is a face subgraph of G if and only if it is a maximal bipartite subgraph of $G[\mathcal{V}(H)]$.*
(2) *A subgraph H of G is a facet subgraph of G if and only if it is a maximal bipartite subgraph of G.*

Proof. First, note that facet subgraphs and maximal bipartite subgraphs are necessarily connected, nontrivial, and spanning, therefore part (2) is a special case of part (1). It is sufficient to establish part (1).

Suppose $H = G_F$ for a proper nonempty face F of $\bar{\nabla}_G$, then, by Lemma 1, there exists an inner normal $\boldsymbol{\alpha} \in \{\mathbf{1}\}^\perp \subset \mathbb{R}^N$ such that

$$\langle \mathbf{x} \, , \, \boldsymbol{\alpha} \rangle = -1 \quad \text{for all } \mathbf{x} \in F \qquad \text{and} \qquad \langle \mathbf{x} \, , \, \boldsymbol{\alpha} \rangle > -1 \quad \text{for all } \mathbf{x} \in \bar{\nabla}_G \setminus F.$$

We will first show G_F is bipartite. Suppose $i_1 \leftrightarrow \cdots \leftrightarrow i_\ell \leftrightarrow i_1$ is a cycle in G_F. Then there are $\lambda_1, \ldots, \lambda_\ell \in \{\pm 1\}$ such that $\lambda_j(\mathbf{e}_{i_j} - \mathbf{e}_{i_{j+1}}) \in F$ for $j = 1, \ldots, \ell$ with $i_{\ell+1} = i_1$. By the above equation,

$$\left\langle \lambda_j(\mathbf{e}_{i_j} - \mathbf{e}_{i_{j+1}}) \, , \, \boldsymbol{\alpha} \right\rangle = -1 \qquad \text{i.e.,} \qquad \left\langle \mathbf{e}_{i_j} - \mathbf{e}_{i_{j+1}} \, , \, \boldsymbol{\alpha} \right\rangle = -\lambda_j \qquad \text{for } j = 1, \ldots, \ell,$$

Summing both sides over $j = 1, \ldots, \ell$ produces

$$0 = \langle \mathbf{0} \, , \, \boldsymbol{\alpha} \rangle = \left\langle \sum_{j=1}^{\ell} \mathbf{e}_{i_j} - \mathbf{e}_{i_{j+1}} \, , \, \boldsymbol{\alpha} \right\rangle = -\sum_{j=1}^{\ell} \lambda_j.$$

Since $\lambda_j \in \{\pm 1\}$ for all j, we can conclude that ℓ must be even. Therefore, any cycle in G_F must be even, i.e., G_F is bipartite.

To show G_F is a maximal bipartite subgraph of $G[\mathcal{V}(G_F)]$, consider a spanning tree T of G_F, which is necessarily a spanning tree of $G[\mathcal{V}(G_F)]$. If B is a bipartite graph such that $G_F < B \leq G[\mathcal{V}(G_F)]$, then any edge $\{i, i'\} \in \mathcal{E}(B) \setminus \mathcal{E}(G_F)$ is also outside T. The fundamental cycle formed by $\{i, i'\}$ and the unique path $i = i_1 \leftrightarrow \cdots \leftrightarrow i_\ell = i'$ in T is contained in B and hence must be an even cycle. That is, ℓ is even. Since the path $i_1 \leftrightarrow \cdots \leftrightarrow i_\ell$ is in $T \leq G_F$, there are $\lambda_1, \ldots, \lambda_{\ell-1} \in \{\pm 1\}$ such that $\lambda_j(\mathbf{e}_{i_j} - \mathbf{e}_{i_{j+1}}) \in F$ for $j = 1, \ldots, \ell - 1$. As in the paragraph above,

$$\langle \mathbf{e}_i - \mathbf{e}_{i'} \, , \, \boldsymbol{\alpha} \rangle = \left\langle \sum_{j=1}^{\ell-1} (\mathbf{e}_{i_j} - \mathbf{e}_{i_{j+1}}) \, , \, \boldsymbol{\alpha} \right\rangle = -\sum_{j=1}^{\ell-1} \lambda_j.$$

Also, by Lemma 1,

$$\langle \pm(\mathbf{e}_i - \mathbf{e}_{i'}) \, , \, \boldsymbol{\alpha} \rangle = \mp \sum_{j=1}^{\ell-1} \lambda_j \geq -1.$$

Recall that $\lambda_j \in \{\pm 1\}$ and ℓ is even. We can conclude that either $\langle +(\mathbf{e}_i - \mathbf{e}_{i'}) \, , \, \boldsymbol{\alpha} \rangle$ or $\langle -(\mathbf{e}_i - \mathbf{e}_{i'}) \, , \, \boldsymbol{\alpha} \rangle$ must be -1, and hence either $+(\mathbf{e}_i - \mathbf{e}_{i'})$ or $-(\mathbf{e}_i - \mathbf{e}_{i'})$ is in also contained in F. That is, $\{i, i'\}$ is in G_F, contradicting our assumption. This shows that G_F is a not contained in any larger bipartite subgraphs of $G[\mathcal{V}(G_F)]$.

For the converse, suppose a connected and nontrivial subgraph $B \leq G$ is a maximal bipartite subgraph of $G[\mathcal{V}(B)]$ with a nontrivial partition $\mathcal{V}(B) = V_+ \cup V_-$. Define $\boldsymbol{\alpha} =$

$(\alpha_1, \ldots, \alpha_N)$ with

$$\alpha_i = \begin{cases} +1/2 & \text{if } i \in V_+ \\ -1/2 & \text{if } i \in V_- \\ 0 & \text{otherwise.} \end{cases}$$

Then

$$\langle\, \mathbf{e}_i - \mathbf{e}_j \,,\, \boldsymbol{\alpha} \,\rangle = \begin{cases} 0 & \text{if } i,j \in V_+ \text{ or } i,j \in V_- \text{ or } i,j \notin V_+ \cup V_- \\ \pm 1 & \text{if } i \in V_\pm \text{ and } j \in V_\mp \\ \pm 1/2 & \text{if exactly one of } i,j \text{ is in } V_+ \cup V_- \end{cases}$$

for any $i, j \in \mathcal{V}(G)$. In particular, since V_+ and V_- partition the vertices of B, which is bipartite, $\langle\, \mathbf{e}_i - \mathbf{e}_j \,,\, \boldsymbol{\alpha} \,\rangle = \pm 1$ for every $\{i, j\} \in \mathcal{E}(B)$. Let

$$F = \{\mathbf{e}_i - \mathbf{e}_j \mid \langle\, \mathbf{e}_i - \mathbf{e}_j \,,\, \boldsymbol{\alpha} \,\rangle = -1\}.$$

By definition, the linear functional $\langle\, \cdot \,,\, \boldsymbol{\alpha} \,\rangle$ attains its minimum over ∇_G on F, and therefore F is a face of ∇_G. Moreover, G_F is a bipartite subgraph of $G[\mathcal{V}(B)]$ that contains B. But B is assumed to be a maximal bipartite subgraph of $G[\mathcal{V}(B)]$, therefore $B = G_F$, i.e., B is a face subgraph. $\square$

Note that the connectedness condition in Theorem 3 is important as disconnected face subgraphs may not be maximal bipartite subgraph of their associated induced subgraphs. For example, Figure 1 shows a face subgraph associated with the 4-cycle $G = C_4$, which is not a maximal bipartite subgraph of its associated induced subgraph $G[\{1, 2, 3, 4\}] = G$. Nonetheless, the argument employed in the above proof still applies to individual connected components of a face subgraph. From this observation we can derive the following generalization to Theorem 3.

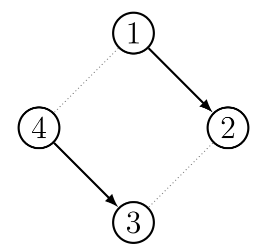

FIGURE 1. A disconnected face subgraph.

Corollary 4. *Let G be a connected graph, and let F be a face of ∇_G. Then each connected component H of G_F is a maximal bipartite subgraph of $G[\mathcal{V}(H)]$.* $\square$

In addition, the above proof shows that for a given maximal bipartite subgraph of G, there is a canonical choice of orientations of the edges that will define a directed facet subgraph and hence a facet.

Corollary 5. *Let B be a maximal bipartite subgraph of a connected graph G with partition of nodes $\mathcal{V}(B) = V_+ \cup V_-$. Then the set*

$$F = \{\mathbf{e}_i - \mathbf{e}_j \mid \{i, j\} \in \mathcal{E}(B), i \in V_- \textit{ and } j \in V_+\}$$

is a facet of $\bar{\nabla}_G$, defined by the facet inner normal $\boldsymbol{\alpha} = (\alpha_1, \ldots, \alpha_N)^\top$ with

$$\alpha_i = \begin{cases} +1/2 & \textit{if } i \in V_+ \\ -1/2 & \textit{if } i \in V_-, \end{cases}$$

and the digraph $\vec{B}$ with edges set

$$\mathcal{E}(\vec{B}) = \{(i, j) \mid \{i, j\} \in \mathcal{E}(B), i \in V_-, j \in V_+\}$$

is its associated directed facet subgraph. $\square$

Note that the naming of the two subsets V_+ and V_- in the partition is arbitrary: permuting the two will result in the facet $-F$ defined by $-\boldsymbol{\alpha}$ associated with the directed facet subgraph $-\vec{B}$. This partition defines a *cut* of the graph G. Such a cut uniquely determines a *cut-set*, which is the set of edges that go across the partition. The construction in the above corollary can be interpreted as a special type of cut-set.

Remark 6. *For a maximal bipartite subgraph $B \leq G$, the canonical choices of edge orientation that produces $\vec{B}$ in Corollary 5 are exactly the edge orientation assignments that would ensure the cut-set (which includes all edges in the bipartite graph B) has a uniform direction across the cut (V_+, V_-) of B, i.e., all directed edges of $\vec{B}$ are from V_- to V_+. In the following, either one of these assignments will simply referred to as a* ***canonical edge orientation*** *for a maximal bipartite subgraph as well as its spanning subgraphs.*

Theorem 3 shows that the map $F \mapsto G_F$ is a surjective map from $\mathcal{F}(\nabla_G)$ to the set of maximal bipartite subgraphs of G. This map is not injective. Indeed, as clarified in Corollary 5, there are at least a pair of canonical choice of facets F and $-F$ associated with any given maximal bipartite subgraph of G, and they correspond to cut-sets having uniform directions. In general, any permutations of the signs of points in F will produce another subset in ∇_G that corresponds to the same (undirected) subgraph of G. However, not all $2^{|F|}$ possibilities will result in facets of ∇_G. In the following, we describe constraints on the possible choices of facets corresponding to a given facet subgraph in terms of oriented cycles. Here, an oriented cycle is a directed cycle with an assigned orientation that is "coherent" in the sense that no vertex is the tail of two edges or the head of two edges.

Theorem 7. *If F is a facet of ∇_G, then for any cycle $\vec{O}$ in G with an assigned orientation,*

$$|\mathcal{E}(\vec{G}_F) \cap \mathcal{E}(\vec{O})| = |\mathcal{E}(\vec{G}_F) \cap \mathcal{E}(-\vec{O})|.$$

Note that G_F being a maximal bipartite subgraph already implies that $|\mathcal{E}(G_F) \cap \mathcal{E}(O)|$ is even for any cycle O in G. This theorem states that the corresponding directed edges in $\mathcal{E}(\vec{G}_F)$ must consist of two subsets of equal size having opposite orientations. Later in this section, we will also show, in Theorem 8, that under an additional dimensional condition the converse is also true.

Proof. Recall that the incidence matrix $Q(\vec{G}_F)$ is totally unimodular [1, Lemma 2.6] [20], and the reduced inner normal $\check{\boldsymbol{\alpha}}$, being the vector satisfying $\check{\boldsymbol{\alpha}}^\top \check{Q}(\vec{G}_F) = -\mathbf{1}^\top$, must be an integer vector. Then $\boldsymbol{\alpha} = (0, \check{\boldsymbol{\alpha}})$ is also an integer vector, and $\pm\langle\, \mathbf{e}_i - \mathbf{e}_j \,,\, \boldsymbol{\alpha} \,\rangle > -1$ is an integer for any $\mathbf{e}_i - \mathbf{e}_j \notin F$. This implies that $\langle\, \mathbf{e}_i - \mathbf{e}_j \,,\, \boldsymbol{\alpha} \,\rangle = 0$ for any $\mathbf{e}_i - \mathbf{e}_j \notin \pm F$.

Suppose G contains a cycle O of length m having edges $i_1 \leftrightarrow i_2 \leftrightarrow \cdots \leftrightarrow i_{m+1}$ with $i_{m+1} = i_1$, and let $E = \mathcal{E}(G_F) \cap \mathcal{E}(O)$. Then $\mathbf{0} = \sum_{r=1}^m \mathbf{e}_{i_r} - \mathbf{e}_{i_{r+1}}$ implies

$$\begin{aligned}
0 &= \left\langle \sum_{r=1}^{m} \mathbf{e}_{i_r} - \mathbf{e}_{i_{r+1}} \,,\, \boldsymbol{\alpha} \right\rangle \\
&= \sum_{\{j,j+1\}\in E} \left\langle \mathbf{e}_{i_{r_j}} - \mathbf{e}_{i_{r_j+1}} \,,\, \boldsymbol{\alpha} \right\rangle + \sum_{\{j,j+1\}\in \mathcal{E}(O)\setminus E} \left\langle \mathbf{e}_{i_{r_j}} - \mathbf{e}_{i_{r_j+1}} \,,\, \boldsymbol{\alpha} \right\rangle \\
&= \sum_{\{j,j+1\}\in E} \left\langle \mathbf{e}_{i_{r_j}} - \mathbf{e}_{i_{r_j+1}} \,,\, \boldsymbol{\alpha} \right\rangle,
\end{aligned}$$

since $\langle \mathbf{e}_i - \mathbf{e}_j \, , \, \boldsymbol{\alpha} \rangle = 0$ for any $\mathbf{e}_i - \mathbf{e}_j \notin \pm F$. Moreover, $\langle \mathbf{e}_i - \mathbf{e}_j \, , \, \boldsymbol{\alpha} \rangle = \pm 1$ for any $\mathbf{e}_i - \mathbf{e}_j \in F$, i.e., each term in the above sum is ± 1. We can conclude that $|E| = |\mathcal{E}(G_F) \cap \mathcal{E}(O)|$ is even.

Let $\vec{O}$ with edges $i_1 \to i_2 \to \cdots \to i_{m+1}$ be the corresponding oriented cycle. Then $\langle \mathbf{e}_{i_{r_j}} - \mathbf{e}_{i_{r_j}+1} \, , \, \boldsymbol{\alpha} \rangle = -1$ implies $(i_{r_j}, i_{r_{j+1}}) \in \mathcal{E}(\vec{G}) \cap \mathcal{E}(\vec{O})$ and $\langle \mathbf{e}_{i_{r_j}} - \mathbf{e}_{i_{r_j}+1} \, , \, \boldsymbol{\alpha} \rangle = 1$ implies $(i_{r_{j+1}}, i_{r_j}) \in \mathcal{E}(\vec{G}) \cap \mathcal{E}(-\vec{O})$. Therefore,

$$|\mathcal{E}(\vec{G}_F) \cap \mathcal{E}(\vec{O})| = |\mathcal{E}(\vec{G}_F) \cap \mathcal{E}(-\vec{O})|.$$

□

Theorem 7 shows the necessary conditions for subset F of $\bar{\nabla}_G$ to be a facet: The intersection between $\vec{G}_F$ and any cycle of G itself must satisfy a balancing condition, i.e., $|\mathcal{E}(\vec{G}_F) \cap \mathcal{E}(\vec{O})| = |\mathcal{E}(\vec{G}_F) \cap \mathcal{E}(-\vec{O})|$ for any oriented cycle $\vec{O}$. By itself, however, this condition is not sufficient to define a facet. For example, the set corresponding to the edges $\mathcal{E}(\vec{O}) \cup \mathcal{E}(-\vec{O})$, for a given oriented cycle $\vec{O}$ in G, clearly satisfies this condition, but it will not form a facet since it contains an interior point $\mathbf{0}$ of ∇_G. In the following, we will show that under additional assumptions, this balancing condition is also a sufficient condition.

Theorem 8. *Let F be a codimension 1 subset of ∇_G such that $\mathbf{0} \notin \operatorname{conv}(F)$. If for any cycle $\vec{O}$ in G with an (coherent) orientation,*

$$|\mathcal{E}(\vec{G}_F) \cap \mathcal{E}(\vec{O})| = |\mathcal{E}(\vec{G}_F) \cap \mathcal{E}(-\vec{O})|,$$

then F is a facet of ∇_G.

Proof. It is sufficient to consider the embedding $\check{\nabla}_G \subset \mathbb{R}^n$ and assume $F \subset \check{\nabla}_G$. Since F is a codimension 1 subset of $\check{\nabla}_G$ that does not contain $\mathbf{0}$ in its convex hull,

$$N - 2 = \dim(F) = \operatorname{rank}(Q(\vec{G}_F)) - 1 = |\mathcal{V}(\vec{G}_F)| - k - 1$$

where $Q(\vec{G}_F)$ is the incidence matrix whose columns are points in F, and k is the number of weakly connected components in $\vec{G}_F$ [1, Theorem 2.3]. Therefore $\vec{G}_F$ is necessarily weakly connected and spanning, and G_F is connected and spanning. Let T be a spanning tree of G_F, then T is also a spanning tree of G. Let $\vec{T}$ be the corresponding directed subgraph of $\vec{G}_F$. By [10, Corollary 3.3], points in $\Delta = \check{\nabla}_{\vec{T}} \subset \check{F}$ form a simplex, and $\check{Q}(\vec{T})$ is nonsingular. Let $\check{\boldsymbol{\alpha}}$ be the unique solution to

$$\check{\boldsymbol{\alpha}}^\top \check{Q}(\vec{T}) = -\mathbf{1}^\top.$$

Then

$$\langle \mathbf{e}_i - \mathbf{e}_j \, , \, \check{\boldsymbol{\alpha}} \rangle = -1 \quad \text{for all } (i,j) \in \vec{T}.$$

Since F is assumed to be a codimension 1 subset in $\check{\nabla}_G$, i.e., $\dim(F) = \dim(\Delta)$, F must be contained in the affine span of Δ. Consequently,

$$\langle \mathbf{e}_i - \mathbf{e}_j \, , \, \check{\boldsymbol{\alpha}} \rangle = -1 \quad \text{for all } \mathbf{e}_i - \mathbf{e}_j \in F.$$

Recall that $\mathbf{0}$ is not contained in the convex hull of F, i.e., F cannot contain both $\pm(\mathbf{e}_i - \mathbf{e}_j)$ for any $\{i, j\}$, so F and $-F$ are disjoint. For any $\mathbf{e}_i - \mathbf{e}_j \in -F$ and hence outside F, it is clear that $\langle \mathbf{e}_i - \mathbf{e}_j \, , \, \check{\boldsymbol{\alpha}} \rangle = +1$.

For any $\mathbf{e}_i - \mathbf{e}_j \in \check{\nabla}_G \setminus (F \cup (-F))$, the corresponding undirected edge $\{i,j\}$ is outside G_F and hence outside T. Consider the fundamental cycle O formed by $\{i,j\}$ and the path $i = i_1 \leftrightarrow \cdots \leftrightarrow i_m \leftrightarrow i_{m+1} = j$ in T. We have

$$\mathbf{e}_i - \mathbf{e}_j = \sum_{j=1}^{m} \mathbf{e}_{i_j} - \mathbf{e}_{i_{j+1}},$$

and there are $\lambda_1, \ldots, \lambda_m \in \{\pm 1\}$ such that $\lambda_j(\mathbf{e}_{i_j} - \mathbf{e}_{j+1}) \in \Delta \subseteq F$. By the assumption that $|\mathcal{E}(\vec{G}_F) \cap \mathcal{E}(\vec{O})| = |\mathcal{E}(\vec{G}_F) \cap \mathcal{E}(-\vec{O})|$, m must be even, and $\lambda_1 + \cdots + \lambda_m = 0$. Therefore,

$$\begin{aligned}\langle\, \mathbf{e}_i - \mathbf{e}_j \,,\, \boldsymbol{\alpha} \,\rangle &= \sum_{j=1}^{m} \langle\, \mathbf{e}_{i_j} - \mathbf{e}_{i_{j+1}} \,,\, \boldsymbol{\alpha} \,\rangle \\ &= \sum_{j=1}^{m} \lambda_j \langle\, \lambda_j(\mathbf{e}_{i_j} - \mathbf{e}_{i_{j+1}}) \,,\, \boldsymbol{\alpha} \,\rangle \\ &= \sum_{j=1}^{m} \lambda_j(-1) = 0.\end{aligned}$$

That is, the linear functional $\langle \,\cdot\,, \boldsymbol{\alpha} \,\rangle$ takes the value of -1 on F, and it is nonnegative on $\nabla_G \setminus F$. Therefore F is a facet.

□

Facets of ∇_G correspond to maximal bipartite subgraphs of G through the map $F \mapsto G_F$. Together, Theorems 7 and 8 give necessary and sufficient conditions on the fiber over a given facet subgraph with respect to this map. Extending this result, the following theorem provides a complete description of the equivalence class of facets corresponding to the same facet subgraph. It will form the foundation for counting and generating facets of ∇_G.

The description makes use of the fundamental cycle vectors and cut-set vectors. For a facet subgraph G_F and a spanning tree T of G_F, let $\vec{T}$ be the corresponding directed subgraph of $\vec{G}_F$. Recall that a facet subgraph is necessarily connected and spanning, so T is also a spanning tree of G itself. Any edge $e \in \mathcal{E}(G) \setminus \mathcal{E}(T)$ induces a fundamental cycle O with respect to T. With an arbitrary assignment of the orientation, the corresponding directed cycle $\vec{O}$ can be expressed as an incidence vector $\mathbf{c}_{\vec{T}}(e) = (c_1, \ldots, c_n)^\top$ with respect to the ordered list of directed edges in $\vec{T}$ so that $-\vec{e}$ corresponds to the point $Q(\vec{T})\mathbf{c}_{\vec{T}}(e) \in \check{\nabla}_G$.

Similarly, fixing an ordering the edges in $\vec{T}$, a cut-set defined by a cut can be expressed as the vector with entries in $\{-1, 0, +1\}$ indicating the direction in which each edge go across the partition (0 for not crossing the partition).

Theorem 9. *For a given maximal bipartite subgraph $B \leq G$ with node partition $V_+ \cup V_- = \mathcal{V}(B)$, let T be a spanning tree of B, and let $\vec{T}$ be the corresponding digraph resulted from the canonical choices of edge orientations (in the sense of Remark 6). There is a bijection between the facets in the equivalence class $\{F \in \mathcal{F}(\check{\nabla}_G) \mid G_F = B\}$ and the set of cut-set vectors $\mathbf{d} \in \{\pm 1\}^n$ of T with respect to the cut (V_+, V_-) satisfying the system*

$$\begin{cases} \mathbf{c}_{\vec{T}}(e)^\top \mathbf{d} &= \pm 1 \quad \text{for } e \in \mathcal{E}(B) \setminus \mathcal{E}(T) \\ \mathbf{c}_{\vec{T}}(e)^\top \mathbf{d} &= \quad 0 \quad \text{for } e \in \mathcal{E}(G) \setminus \mathcal{E}(B) \end{cases} \tag{1}$$

Note that the $\pm$ sign is the consequence of the ambiguity in the orientation assignment for a given fundamental cycle.

Proof. Since B, being a maximal bipartite subgraph of G, must be spanning, T is also a spanning tree of G, and (V_+, V_-) is also a partition of $\mathcal{V}(G)$. Recall that $\vec{T}$, the canonical edge orientation assignment for T (Remark 6) has the edge set

$$\mathcal{E}(\vec{T}) = \{(i,j) \mid \{i,j\} \in \mathcal{E}(T),\, i \in V_-,\, j \in V_+\}.$$

Let $\mathbf{d} \in \{\pm 1\}^n$ be a cut-set vector satisfying the system of equations (1), and let $D = \operatorname{diag}(\mathbf{d})$. Then there exists a vector $\boldsymbol{\alpha} \in \mathbb{R}^N$ such that $\boldsymbol{\alpha}^\top Q(\vec{T}) = -\mathbf{d}$, i.e.

$$\boldsymbol{\alpha}^\top Q(\vec{T}) D = -\mathbf{1}.$$

Define Δ' to be the set of points that are the columns of $Q(\vec{T})\operatorname{diag}(\mathbf{d})$, then $G_{\Delta'} = T$ and thus Δ' is a codimension-1 simplex in $\bar{\nabla}_G$. Moreover, the above equations shows that

$$\langle\, \mathbf{x}\,,\, \boldsymbol{\alpha}\,\rangle = -1 \quad \text{for any } \mathbf{x} \in \Delta'.$$

If $T \neq B$, then any edge $e \in \mathcal{E}(B) \setminus \mathcal{E}(T)$ determines a fundamental cycle with respect to T represented by vector $\mathbf{c} = \mathbf{c}_T(e)$ such that e corresponds to a point

$$\mathbf{x} = -Q(\vec{T})\mathbf{c}.$$

By assumption (1), $\mathbf{c}^\top \mathbf{d} = \pm 1$. Therefore,

$$\boldsymbol{\alpha}^\top \mathbf{x} = \boldsymbol{\alpha}^\top(-Q(\vec{T})\mathbf{c}) = -\boldsymbol{\alpha}^\top Q(\vec{T}) D D \mathbf{c} = \mathbf{1}^\top D \mathbf{c} = \mathbf{d}^\top \mathbf{c} = \pm 1.$$

Similarly, for any $e \in \mathcal{E}(G) \setminus \mathcal{E}(B)$, the fundamental cycle with respect to T is represented by a vector vector $\mathbf{c} = \mathbf{c}_T(e)$ such that e corresponds to a point $\mathbf{x} = -Q(\vec{T})\mathbf{c}$. By assumption (1), $\mathbf{c}^\top \mathbf{d} = 0$. Following the same calculations above,

$$\boldsymbol{\alpha}^\top \mathbf{x} = \boldsymbol{\alpha}^\top(-Q(\vec{T})\mathbf{c}) = -\boldsymbol{\alpha}^\top Q(\vec{T}) D D \mathbf{c} = \mathbf{1}^\top D \mathbf{c} = \mathbf{d}^\top \mathbf{c} = 0.$$

We have shown $\langle\, \mathbf{x}\,,\, \boldsymbol{\alpha}\,\rangle$ is -1 for all $\mathbf{x}$ in the codimension-1 simplex Δ' of $\bar{\nabla}_G$ and ± 1 or 0 for any non-interior point in $\bar{\nabla}_G$. Therefore, $\boldsymbol{\alpha}$ defines a unique facet $\operatorname{aff}(\Delta') \cap \bar{\nabla}_G \in \mathcal{F}(\nabla_G)$. That is, each solution $\mathbf{d}$ to the system (1), determined a unique facet of $\bar{\nabla}_G$.

Conversely, any facet $F \in \mathcal{F}(\bar{\nabla}_G)$ such that $G_F = B \geq T$ must contain the subset $\{d_1\mathbf{x}_1, \dots, d_n\mathbf{x}_n\}$ for some $\mathbf{d} = (d_1, \dots, d_n) \in \{\pm 1\}^n$, where $\{\mathbf{x}_1, \dots, \mathbf{x}_n\} = \bar{\nabla}_{\vec{T}}$. The vector $\mathbf{d}$ is uniquely determined by the choice of $\vec{T}$. By Theorem 7, $\mathbf{d}$ must satisfy the equations in (1). That is, each facet of $\bar{\nabla}_G$ corresponds to a unique solution $\mathbf{d}$ to the system (1). □

D'Alì, Delucchi, and Michałek showed that for a connected bipartite graph G, $|\mathcal{F}(\nabla_G)$ is bounded by 2^{N-1} [10, Corollary 4.6]. It is then noted that this upper bound no longer hold when the graph is not bipartite. From the above proof, we can derive a refinement of this result: this upper bound always hold for the number of facets in an equivalence class of facets associated with a given facet subgraph.

Corollary 10. *For a given connected graph G and a facet $F \in \mathcal{F}(\nabla_G)$,*

$$|\,\{F' \in \mathcal{F}(\nabla_G) \mid G_{F'} = G_F\}\,| \leq 2^{N-1}.$$

With this, we can derive an upper bound for the total number of facets.

Corollary 11. *For a given connected graph G,*

$$|\,\mathcal{F}(\nabla_G)\,| \leq \beta \cdot 2^{N-1},$$

where β is the number of maximal bipartite subgraphs that G has.

In the special case when G is bipartite, the only facet subgraph, i.e., the unique maximal bipartite subgraph, is G itself, and the result reduces to the previously established upper bound [10, Corollary 4.6].

Now, we provide connections between the geometric properties of faces of ∇_G and the graph-theoretical properties of their corresponding face subgraphs. Recall that the *cyclomatic number* of a graph G is the minimum number of edges that can be deleted from G such that the resulting graph is acyclic.

Theorem 12. *For a proper face F of ∇_G,*

(i) F is independent if and only if G_F is a forest;
(ii) F is a circuit if and only if G_F is a chordless cycle;
(iii) $\dim(F) = |\mathcal{V}(G_F)| - k - 1$ where k is the number of connected components in G_F; and
(iv) $\operatorname{corank} F$ equals the cyclomatic number of G_F.

It is worth noting that if G_F is spanning, then the codimension and the corank of F are exactly the Betti number of G_F.

Proof. (i) Since every proper face of ∇_G is contained in a facet, without loss of generality, we can assume F is a facet. Suppose G_F contains a cycle O with edges $i_1 \leftrightarrow \cdots \leftrightarrow i_m \leftrightarrow i_1$, then, by Theorem 7, it must be an even cycle, and there exist $\lambda_1, \ldots, \lambda_m \in \{\pm 1\}$ with $\sum_{j=1}^{m} \lambda_j = 0$ such that

$$\lambda_j(\mathbf{e}_{i_j} - \mathbf{e}_{i_{j+1}}) \in F$$

for all j. This gives us the affine dependence relation

$$\sum_{j=1}^{m} \lambda_j(\lambda_j(\mathbf{e}_{i_j} - \mathbf{e}_{i_{j+1}})) = \sum_{j=1}^{m} \mathbf{e}_{i_j} - \mathbf{e}_{i_{j+1}} = \mathbf{0}$$

with the coefficients $\lambda_1, \ldots, \lambda_m$. Therefore F itself cannot be independent.

Conversely, if G_F is a forest, then the incidence matrix $Q(\vec{G}_F)$, whose columns are points in F, has full column rank [1, Lemma 2.5] [20]. Therefore F is independent.

(ii) If F is a circuit, then F is dependent by definition. By part (i), G_F contains a cycle and the corresponding subset of points in F is dependent. However, the circuit F, being a minimal affinely dependent set, must be exactly this set. Therefore G_F is exactly this cycle.

Conversely, if F is not a circuit, then either F is independent or F contains a proper dependent subset F'. Again by part (i), G_F is either a forest or it contains a strictly smaller cycle, and thus G_F is not a chordless cycle.

(iii) Let $Q(\vec{G}_F)$ be the incidence matrix of $\vec{G}_F$. Then

$$\dim(F) = \operatorname{rank}(Q(\vec{G}_F)) - 1 = |\mathcal{V}(G_F)| - k - 1$$

where k is the number of connected components in G_F.

(iv) Let μ and k be the cyclomatic number and number of connected components of G_F respectively. By part (iii) we have

$$\begin{aligned}\mu &= |\mathcal{E}(G_F)| - |\mathcal{V}(G_F)| + k \\ &= |F| - (\dim(F) + 1) \\ &= \operatorname{corank}(F).\end{aligned}$$

$\square$

Remark 13. *Note that the results in Theorem 12 extend trivially to subsets of facets, including subsets that do not form faces, if we follow the convention that the empty set is independent and the subgraph containing no edge is a forest. With this observation, Theorem 12 highlights the connection through which independent subsets correspond to forests, dependent subsets correspond to graphs with cycles, and circuits correspond to chordless cycles. A more precise characterization emerges from the point of view of matroid theory.*

Recall that a matroid consists of a finite ground set *together with a family of its subsets, called* independent sets*, that satisfies the independence axioms (a) the empty set is independent; (b) any subset of an independent set is independent; and (c) for two independent sets A and B with $|A| < |B|$, $A \cup \{b\}$ is independent for some $b \in B$. Subsets of the ground set that are not independent are* dependent sets*. A maximally independent set is a* basis *while a minimally dependent set is a* circuit*. Two matroid structures appear naturally in this context, and theorem 12 shows that they are essentially the mirror images of one another.*

Taking a given facet F of ∇_G to be the ground set and its (affinely) independent subsets (including $\varnothing$) to be independent subsets, we have a matroid structure. On the other hand, building on the ground set $E_F = \mathcal{E}(G_F)$, we can also construct a matroid where the independent elements are subsets of edges, including the empty set, that does not contain a cycle. In this setup, a basis is a spanning tree, and a circuit is a chordless cycle. Theorem 12 shows that the map $X \mapsto \mathcal{E}(G_X)$ preserves matroid properties.

In the matroid-theoretic context, the cyclomatic number of a graph is also known as the *corank* of a graph, which is preserved in the in the face-subgraph correspondence, i.e., the corank of a face F of ∇_G (as a point configuration) is the same as the corank of G_F (as a graph). Therefore, in the following, we will refer to graphs of cyclomatic number c simply as corank-c graphs.

Combining Theorems 3 and 12 part (i), we can conclude that ∇_G is simplicial (i.e., all of its facets are simplices) if and only if all maximal bipartite subgraphs of G are trees.

Corollary 14. *∇_G is simplicial if and only if G is connected and has no even cycles.* $\square$

4.3. **Applications to algebraic Kuramoto equations.** Facets of ∇_G play important roles in the study of algebraic Kuramoto equations [3, 4, 7], which has attracted interests from electric engineering, biology, and chemistry. The original Kuramoto equations models the synchronization behaviors of a network of coupled oscillators [15], which can be represented by a weighted graph G with the nodes $\mathcal{V}(G) = \{0, \ldots, n\}$ representing the oscillators, the edges $\mathcal{E}(G)$ representing the connections among the oscillators, and the weights $K = \{k_{ij}\}$ representing the *coupling strength* along the edges. Each oscillator i has its own natural frequency ω_i. The dynamics of the network can be described by the differential equations

$$\frac{d\theta_i}{dt} = \omega_i - \sum_{j \in \mathcal{N}_G(i)} k_{ij} \sin(\theta_i - \theta_j), \quad \text{for } i = 0, \ldots, n, \tag{2}$$

where each $\theta_i \in [0, 2\pi)$ is the phase angle that describes the status of the i-th oscillator, and $\mathcal{N}_G(i)$ is the set of its neighbors. *Frequency synchronization* occurs when the competing forces reach equilibrium and all oscillators are tuned to the same frequency, i.e., $\frac{d\theta_i}{dt} = c$ for a common constant c for all i. They are precisely the solutions to the system of equations

$$\omega_i - \sum_{j \in \mathcal{N}_G(i)} k_{ij} \sin(\theta_i - \theta_j) = c \quad \text{for } i = 1, \dots, n \tag{3}$$

in the variables $\theta_1, \dots, \theta_n$. Here $\theta_0 = 0$ is fixed as the reference phase angle. With the substitution $x_i := e^{\mathbf{i}\theta_i}$ ($x_0 = 1$), (3) can be transformed into the algebraic system

$$F_{G,i}(x_1, \dots, x_n) = \omega_i - c - \sum_{j \in \mathcal{N}_G(i)} \frac{k_{ij}}{2\mathbf{i}} \left(\frac{x_i}{x_j} - \frac{x_j}{x_i} \right) = 0 \quad \text{for } i = 1, \dots, n. \tag{4}$$

$F_G = (F_{G,1}, \dots, F_{G,n})$ is a system of n Laurent polynomial equations in the n nonzero complex variables $\mathbf{x} = (x_1, \dots, x_n) \in (\mathbb{C}^*)^n = (\mathbb{C} \setminus \{0\})^n$.

Considering F_G as a column vector, then for any nonsingular $n \times n$ matrix R, the systems $F_G^R = R \cdot F_G$ and F_G have the same zero set. For generic choices of the matrix R, there is no complete cancellation of the terms, and thus F_G^R is of the form

$$F_{G,k}^R = c_k^R - \sum_{\{i,j\} \in \mathcal{E}(G)} \left(a_{ijk}^R \frac{x_i}{x_j} + a_{jik}^R \frac{x_j}{x_i} \right) \quad \text{for } k = 1, \dots, n, \tag{5}$$

where c_k^R and a_{ijk}^R are the resulting nonzero coefficients after collection of similar terms. This is the *algebraic Kuramoto system* in its *unmixed form*. To see the connections to adjacency polytopes more clearly, we shall use the vector exponent notation

$$(x_1, \dots, x_n)^{\begin{bmatrix} a_1 \\ \vdots \\ a_n \end{bmatrix}} = x_1^{a_1} \cdots x_n^{a_n}.$$

Then we can write (5) as

$$F_{G,k}^R(\mathbf{x}) = \sum_{\mathbf{a} \in \check{\nabla}_G} c(\mathbf{a})\, \mathbf{x}^{\mathbf{a}} \quad \text{for } k = 1, \dots, n,$$

where the function $c : \check{\nabla}_G \to \mathbb{C}$ captures the coefficients. That is, $\check{\nabla}_G$ is exactly the support of the unmixed form of the algebraic Kuramoto system. Facets and faces, in general, of $\check{\nabla}_G$ play particular important roles in the study of this algebraic system. In the following, we highlight three them, namely the roles in toric deformation homotopy method (section 4.3.1), root counting (section 4.3.2), and construction of homogeneous coordinates (section 4.3.3).

4.3.1. *Toric deformation homotopy.* The toric deformation homotopy for unmixed algebraic Kuramoto equations is a specialized *polyhedral homotopy* [14] construction for locating *all* complex zeros of (5), which includes *all* frequency synchronization configurations. Utilizing the topological information extracted from the underlying graph, this homotopy construction has the potential to avoid the computationally expensive preprocessing steps associated with polyhedral homotopy (e.g. mixed cell computations). In the most basic form, it is defined by the function $H_G : \mathbb{C}^n \times \mathbb{C} \to \mathbb{C}^n$ with $H_G(\mathbf{x}, t) = (H_{G,1}, \dots, H_{G,n})$ given by

$$H_{G,k} = \sum_{\mathbf{a} \in \check{\nabla}_G} c(\mathbf{a})\, \mathbf{x}^{\mathbf{a}} t^{\omega(\mathbf{a})} \quad \text{for } k = 1, \dots, n, \quad \text{where } \omega(\mathbf{a}) = \begin{cases} 0 & \text{if } \mathbf{a} = \mathbf{0} \\ 1 & \text{otherwise.} \end{cases} \tag{6}$$

Clearly, $H_G(\mathbf{x}, 1) = F_G^R(\mathbf{x})$. As t varies between 0 and 1 within the interval $(0, 1)$, $H_G(\mathbf{x}, t)$ represents a smooth deformation of the system F_G^R, and the corresponding complex roots also vary smoothly, forming smooth paths reaching *all* complex zeros of F_G^R [3, 14].

The starting points of the smooth paths, however, are not well defined, as the limit points of these paths as $t \to 0$ are not contained in $(\mathbb{C}^*)^n$. Yet, with the change of variables

$$x_k = y_k t^{\alpha_k} \quad \text{for } k = 1, \dots, n,$$

where $\check{\boldsymbol{\alpha}} = (\alpha_1, \dots, \alpha_n)$ is a normalized inner normal of a facet $F \in \mathcal{F}(\check{\nabla}_G)$. The limit point of certain paths, in the y-coordinates, are exactly the $(\mathbb{C}^*)$-solutions to the subsystem

$$0 = \sum_{\mathbf{a} \in F \cup \{\mathbf{0}\}} c(\mathbf{a})\, \mathbf{x}^{\mathbf{a}} \quad \text{for } k = 1, \dots, n$$

define by the facet F. As the pair $(F, \check{\boldsymbol{\alpha}})$ run through the set of facets and their corresponding normalized inner normals, the solutions of the subsystems of the above form include limit points, in the y-coordinate, of *all* paths defined by $H_{G,k} = 0$. Therefore, explicit descriptions to the facets of $\check{\nabla}_G$ as well as their inner normals are crucially important in bootstrapping the toric deformation homotopy method for solving the Kuramoto equations.

4.3.2. *Facets systems and the root counting problem.* A closely related application is the root counting problem for the algebraic Kuramoto equations (5). It is shown that for generic choices of the coefficients, the total complex root count for algebraic Kuramoto equations induced by cycles and trees is exactly the adjacency polytope bound. When there are algebraic relations among the coefficients, the actual root count may be strictly less. An algebraic certificate for such decrease in root count is provided by "face systems". For a positive-dimensional face F of $\check{\nabla}_G$, the corresponding *face system* of (5) is given by

$$0 = \sum_{\mathbf{a} \in F} c(\mathbf{a})\, \mathbf{x}^{\mathbf{a}} \quad \text{for } k = 1, \dots, n \tag{7}$$

By Bernshtein's Second Theorem [2], if (7) has nontrivial solutions ($\mathbb{C}^*$-solutions), then the root count for (5) is strictly less than the adjacency polytope bound. Consequently, the descriptions of faces, especially facets, of $\check{\nabla}_G$ given in Theorems 3 and 9 provide us a foundation for studying the root count of the algebraic Kuramoto equations (5).

4.3.3. *Construction of homogeneous coordinates.* One issue users of homotopy continuation methods have to face is the existence of divergent paths, e.g., solution paths defined by (6) that do not have limit points, as $t \to 1$, in the work space $\mathbb{C}^n$. A common solution is to compactify the work space. The homogeneous coordinates, a special case of Cox's homogeneous ring [9], provide the most general construction for achieving this goal. Even though the use of homogeneous coordinates tends to introduce a large number of auxiliary variables and hence impractical in actual calculations, they remain important tools for theoretical analysis of algebraic Kuramoto equations. The foundation of homogeneous coordinates construction is the full description of facets $\mathcal{F}(\nabla_G)$ and their inner normals.

Let $m = |\mathcal{F}(\check{\nabla}_G)|$, and let $\boldsymbol{\alpha}_1, \ldots, \boldsymbol{\alpha}_m$ be the primitive inner normals for the facets of $\check{\nabla}_G$. Define the matrix V to be the $m \times n$ matrix whose rows are $\boldsymbol{\alpha}_1^\top, \ldots, \boldsymbol{\alpha}_m^\top$. Let $\mathbf{h} = (h_1, \ldots, h_m)^\top$ be the column vector with entries

$$h_i = \min_{\mathbf{x} \in \check{\nabla}_G} \langle \mathbf{x} \, , \, \boldsymbol{\alpha}_i \rangle.$$

The homogenization of $F^R_{G,k}$ (5) is the polynomial $\hat{F}^R_{G,k}(\mathbf{y})$ in the complex variables $\mathbf{y} = (y_1, \ldots, y_m)$ given by

$$\hat{F}^R_{G,k}(\mathbf{y}) = \sum_{\mathbf{a} \in \check{\nabla}_G} c(\mathbf{a}) \, \mathbf{y}^{V\mathbf{a} - \mathbf{h}}.$$

The system $\hat{F}^R_G = (\hat{F}^R_{G,1}, \ldots, \hat{F}^R_{G,n})$ represents a lifting of the system (5) to a compact topological space (a compact toric variety). Consequently, each solution path defined by the homotopy (6) has a limit point corresponding to an equivalence class of zero of $\hat{F}^R_G$ in this compact space, even if it has no limit point in $\mathbb{C}^n$.

5. An example: Joining two cycles along a shared edge

D'Alì, Delucchi, and Michałek showed that for a graph formed by joining two bipartite graphs along an edge, the number of facets of the associated adjacency polytope (symmetric edge polytope) is $\frac{1}{2} f_1 f_2$ where f_1 and f_2 are the number facets in the adjacency polytopes associated with the two bipartite subgraphs respectively [10, Proposition 4.10]. In the following we explore the more general situation in which one of the subgraph is not bipartite.

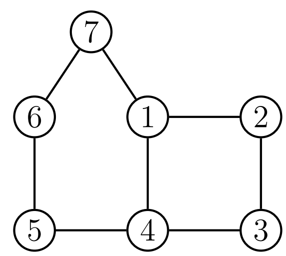

FIGURE 2. A graph formed by joining a 4-cycle and a 5-cycle along an edge

Figure 2 shows a graph G formed by joining a 4-cycle and a 5-cycle along a single shared edge. G is not bipartite as it contains an odd cycle. As we will calculate, the facet count described above ([10, Proposition 4.10]) no longer applies, but Theorem 9 provides a concrete recipe for calculating the number of facets and describing the combinatorial structure of the facets.

Graph G contains 7 maximal bipartite subgraphs, which are shown in Figure 3. As established in Theorem 3, they correspond to the five equivalence classes of facets in $\mathcal{F}(\nabla_G)$. Among these subgraphs, 3 of them are trees (Figure 3a), and, according to Theorem 12 part (i) they correspond to corank-0 (simplicial) facets. The other 4 each contains a unique 4-cycle (Figure 3b), and, according to Theorem 12 part (iv) they correspond to corank-1 facets.

We pick a corank-0 facet subgraph (in Figure 3a), a spanning tree of this subgraph, and an assignment of edge orientations. These choices are shown in Figure 4. Up to a recording of the edges, the two fundamental cycles can be expressed as vectors $[+1, -1, +1, -1, +1, -1]$ and $[0, 0, +1, -1, +1, -1]$. Therefore the defining equation (1) in Theorem 9 for the parametrization of the facets in this equivalence class is

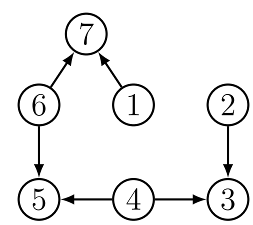

FIGURE 4. A corank-0 facet subgraph and its spanning tree.

$$\begin{bmatrix} +1 & -1 & +1 & -1 & +1 & -1 \\ 0 & 0 & +1 & -1 & +1 & -1 \end{bmatrix} \mathbf{d} = \begin{bmatrix} 0 \\ 0 \end{bmatrix}$$

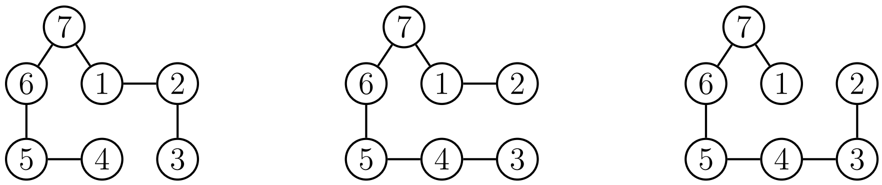

(A) Corank-0 facet subgraphs of G

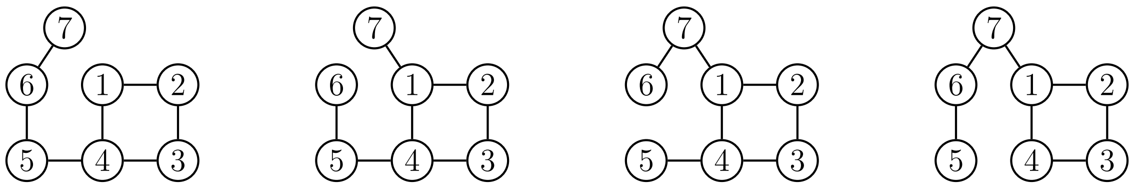

(B) Corank-1 facet subgraphs of G

FIGURE 3. Facet subgraphs (maximal bipartite subgraphs) of G

in the unknowns $\mathbf{d} = (d_1, \ldots, d_6)^\top \in \{\pm 1\}^6$. This equation is equivalent to

$$\begin{bmatrix} +1 & -1 & 0 & 0 & 0 & 0 \\ 0 & 0 & +1 & -1 & +1 & -1 \end{bmatrix} \mathbf{d} = \begin{bmatrix} 0 \\ 0 \end{bmatrix}.$$

From this we can see that (d_1, d_2) and (d_3, d_4, d_5) can be described independently, and there are two possible choices for (d_1, d_2), namely $(+1, +1)$ and $(-1, -1)$. Similarly, there are 6 possible choices for (d_3, d_4, d_5, d_6):

$$\begin{array}{lll} (+1,+1,+1,+1) & (+1,+1,-1,-1) & (+1,-1,-1,+1) \\ (-1,-1,+1,+1) & (-1,-1,-1,-1) & (-1,+1,+1,-1). \end{array}$$

Altogether, there are 12 possible choice for the vector $\mathbf{d} \in \{\pm 1\}^6$ for the equation (1). These produce 12 distinct facets in the equivalence class of facets corresponding to a corank-0 maximal bipartite subgraph of G shown in Figure 3a.

Similarly, we pick a facet subgraph G_F of corank 1 in Figure 3b, a spanning tree T of this subgraph, and a canonical assignment of edge orientations $\vec{T}$. These choices are shown in Figure 5, where the dotted edge is in $\vec{G}_F$ but not in $\vec{T}$. With respect to this choice, and up to a reordering of the edges in $\vec{T}$, the two fundamental cycles can be expressed as vectors $[-1, -1, +1, 0, 0, 0]$ and $[0, 0, +1, -1, +1, -1]$. Therefore the fundamental cycle equations are

$$\begin{bmatrix} -1 & -1 & +1 & 0 & 0 & 0 \\ 0 & 0 & +1 & -1 & +1 & -1 \end{bmatrix} \mathbf{d} = \begin{bmatrix} \pm 1 \\ 0 \end{bmatrix}.$$

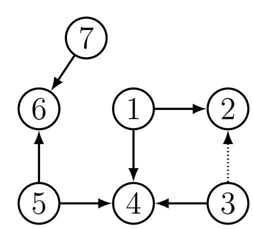

FIGURE 5. A corank-1 facet subgraph and its spanning tree.

Through direct calculations we can see there are 18 solutions for $\mathbf{d} \in \{\pm 1\}^6$ corresponding to the 18 facets in the equivalence class.

The same argument can be applied to each of the 4 corank-1 facet subgraphs in Figure 3b. Therefore there are 72 corank-1 facets in $\mathcal{F}(\nabla_G)$.

Altogether are are $36 + 72 = 108$ facets in $\mathcal{F}(\nabla_G)$. Among them, 36 facets are simplicial, and the remaining 72 facets are (affinely) dependent and are of corank 1.

The calculation shown in this concrete example can be easily generalized to graphs formed by joining an even cycle and an odd cycle along a shared edge. The counting argument involved makes use of the following elementary formulas from combinatorics.

Lemma 15. *For a positive integer n, there are exactly $\binom{2n}{n}$ distinct choices of vectors $\mathbf{d} \in \{\pm 1\}^{2n}$ that satisfies the equation*

$$\begin{bmatrix} \overbrace{+1 \ \cdots \ +1}^{n} & \overbrace{-1 \ \cdots \ -1}^{n} \end{bmatrix} \mathbf{d} = 0.$$

Lemma 16. *For a positive integer n, there are exactly $\binom{2n}{n-1}$ distinct choices of vectors $\mathbf{d} \in \{\pm 1\}^{2n}$ that satisfies the equation*

$$\begin{bmatrix} \overbrace{+1 \ \cdots \ +1}^{n} & \overbrace{-1 \ \cdots \ -1}^{n} \end{bmatrix} \mathbf{d} = 2.$$

Proof. The solutions $\mathbf{d} = (d_1, \ldots, d_{2n})^\top \in \{\pm 1\}^{2n}$ to this equation correspond to the different ways of choosing only i entries among $(d_1, \ldots, d_n)$ and $i+1$ entries among $(d_{n+1}, \ldots, d_{2n})$ to be -1 for $i = 0, \ldots, n-1$. Therefore, by applying the Vandermonde identity, the total number of possibilities is

$$\sum_{i=0}^{n-1} \binom{n}{i} \binom{n}{i+1} = \binom{2n}{n-1}. \qquad \square$$

Proposition 17. *Let G be the graph formed by joining two cycles of size $2m_1$ and $2m_2 + 1$ respectively along a shared edge. Then the number of facets ∇_G has is*

$$\left[(2m_1 - 1) \binom{2m_1 - 2}{m_1 - 1} + (2m_2) \binom{2m_1 - 1}{m_1} \right] \binom{2m_2}{m_2}$$

Proof. First note that G contains $N = 2m_1 + 2m_2 - 1$ nodes and $2m_1 + 2m_2$ edges. Since G has a unique even cycle, by Theorem 3 and Theorem 12, the coranks of facets of ∇_G are either 0 or 1. We shall count them separately.

We first count the corank-0 facets. By Theorem 12 part (iv), the facet subgraph of G associated with a corank-0 facet must be a spanning tree of G that is also a maximal bipartite subgraph of G. G has exactly $2m_1 - 1$ such spanning trees, obtained by deleting the edge shared by the $2m_1$-cycle and the $(2m_2 + 1)$-cycle and by deleting exactly one additional edge of the $2m_1$-cycle (exemplified in Figure 3a). Note that these corank-0 facet subgraphs are all paths of the same length, hence isomorphic to one another. Up to a re-indexing of the $n = 2m_1 + 2m_2 - 2$ edges, the counting arguments for each of these spanning trees are identical. It is therefore sufficient to calculate the number of facets associated with a single spanning tree (path) T of G that is also a maximal bipartite subgraph of G.

There are exactly two edges in $\mathcal{E}(G) \setminus \mathcal{E}(T)$ — the edge shared by the two cycles and another edge of the even cycle. Let $\vec{T}$ be the corresponding digraph resulting from the canonical choice of edge orientations as described in Remark 6. The fundamental cycle C induced by the first edge includes all edges of the odd cycle, and the other fundamental cycle

C' includes all edges of $\vec{T}$. Therefore, equation (1) is of the form

$$\left[\begin{array}{cccccccccc} \multicolumn{5}{c}{\overbrace{\hphantom{0 \quad 0 \quad \cdots \quad 0 \quad 0}}^{2m_1-2}} & \multicolumn{5}{c}{\overbrace{\hphantom{+1 \quad -1 \quad \cdots \quad +1 \quad -1}}^{2m_2}} \\ 0 & 0 & \cdots & 0 & 0 & +1 & -1 & \cdots & +1 & -1 \\ +1 & -1 & \cdots & +1 & -1 & +1 & -1 & \cdots & +1 & -1 \end{array}\right] \mathbf{d} = \begin{bmatrix} 0 \\ 0 \end{bmatrix}, \tag{8}$$

and the number of facets whose facet subgraph is T is exactly the total number of solutions $\mathbf{d} = (d_1, \ldots, d_n)^\top \in \{\pm 1\}^n$ to the above equation. Note that $(d_1, \ldots, d_{2m_1-2}) \in \{\pm 1\}^{2m_1-2}$ and $(d_{2m_1-1}, \ldots, d_n) \in \{\pm 1\}^{2m_2}$ can be solved independently.

The constraints on $(d_1, \ldots, d_{2m_1-2}) \in \{\pm 1\}^{2m_1-2}$ in (8) is equivalent to $d_1 - d_2 + d_3 - \cdots + d_{2m_1-3} - d_{2m_1-2} = 0$. By Lemma 15, the total number of such choices for $(d_1, \ldots, d_{2m_1-2}) \in \{\pm 1\}^{2m_1-2}$ is $\binom{2m_1-2}{m_1-1}$. Similarly, the constraints on $(d_{2m_1-1}, \ldots, d_n) \in \{\pm 1\}^{2m_2}$ in (8) is equivalent to $d_{2m_1-1} - d_{2m} + d_{2m+1} - \cdots + d_{n-1} - d_n = 0$, and, by Lemma 15, the number of $\{\pm 1\}$-solutions is $\binom{2m_2}{m_2}$. Therefore, the number of solutions $\mathbf{d} \in \{\pm 1\}^n$ to (8), being the product of solutions for $(d_1, \ldots, d_{2m_1-2}) \in \{\pm 1\}^{2m_1-2}$ and $(d_{2m_1-1}, \ldots, d_n) \in \{\pm 1\}^{2m_2}$ is $\binom{2m_1-2}{m_1-1}\binom{2m_2}{m_2}$. That is, by Theorem 9, the number of facets whose facet subgraph is T is given by

$$|\{F \in \mathcal{F}(\nabla_G) \mid G_F = T\}| = \binom{2m_1-2}{m_1-1}\binom{2m_2}{m_2}.$$

Recall that there are $2m_1 - 1$ distinct spanning tree that are maximal bipartite subgraphs of G, each having the same number of associated facets, therefore, the total number of corank-0 facets ∇_G has is

$$(2m_1 - 1)\binom{2m_1-2}{m_1-1}\binom{2m_2}{m_2}. \tag{9}$$

Now we count the corank-1 facets. Since G contains a unique even cycle, by Theorem 3 and Theorem 12 part (iv), the facet subgraph G_F of a facet $F \in \mathcal{F}(\nabla_G)$ of corank 1, being a maximal bipartite subgraph of G of cyclomatic number 1, must contain this even cycle as well as all except one edge of the odd cycle. Therefore, there are exactly $2m_2$ distinct subgraphs of G corresponding to facets of corank 1, as exemplified in Figure 3b. As in the previous case, since all these corank-1 facet subgraphs have the same fundamental cycles, up to a re-indexing of edges, the counting arguments for each of these subgraph are identical, and it is therefore sufficient to calculate the number of facets associated with a single corank-1 subgraph $B < G$.

Fix any spanning tree $T < B$, and let $\vec{T}$ be the corresponding digraph resulted from the canonical choice of edge orientations. There is only one edge in $\mathcal{E}(B) \setminus \mathcal{E}(T)$, and the corresponding fundamental cycle involves all edges of the even cycle (as shown in Figure 5). Up to a re-indexing of the edges, the corresponding fundamental cycle vector can be expressed as $[+1, -1, +1, \ldots, -1, +1, 0, \ldots, 0]$ with the last $2m_2 - 1$ coordinates being zero.

Similarly, there is only one edge in $\mathcal{E}(G) \setminus \mathcal{E}(B)$, and the corresponding fundamental cycle involves all edges of the $(2m_2 + 1)$-cycle. Its fundamental cycle vector can be expressed as $[0, \ldots, 0, +1, -1, +1, \ldots, -1, +1]$ with the first $2m_1 - 2$ coordinates being zero. Therefore, equation (1) is of the form

$$\begin{bmatrix} \overbrace{+1 \quad \cdots \quad -1}^{2m_1-2} & \overbrace{+1 \quad 0 \quad \cdots \quad 0 \quad 0}^{2m_2} \\ 0 \quad \cdots \quad 0 & +1 \quad -1 \quad \cdots \quad +1 \quad -1 \end{bmatrix} \mathbf{d} = \begin{bmatrix} \pm 1 \\ 0 \end{bmatrix}, \tag{10}$$

and its solutions $\mathbf{d} = (d_1, \ldots, d_n)^\top \in \{\pm 1\}^n$ are in one-to-one correspondence with the facets whose facet subgraph is B.

We can solve for $(d_{2m_1-1}, d_{2m_1}, \ldots, d_n) \in \{\pm 1\}^{2m_2}$, subjects to the constraint $d_{2m_1-1} - d_{2m_1}, \ldots, +d_n = 0$, independently. Following the counting argument used in the previous case, we can verify that there are exactly $\binom{2m_2}{m_2}$ distinct choices for $(d_{2m_1-1}, d_{2m_1}, \ldots, d_n) \in \{\pm 1\}^{2m_2}$.

The choices of $(d_1, \ldots, d_{2m_1-2})$, however, depends on the value of d_{2m_1-1}, since they are related by the equation $d_1 - d_2 + \cdots - d_{2m_1-2} + d_{2m_1-1} = p$, where $p \in \{\pm 1\}$. We consider the two cases depending on the sign of d_{2m_1-1}/p.

If $p = d_{2m_1-1}$, the equation is equivalent to $d_1 - d_2 + \cdots - d_{2m_1-2} = 0$, and there are exactly $\binom{2m_1-2}{m_1-1}$ distinct choices for $(d_1, \ldots, d_{2m_1-2}) \in \{\pm 1\}^{2m_1-2}$. If $p = -d_{2m_1-1}$, the equation is equivalent to $d_1 - d_2 + \cdots - d_{2m_1-2} = 2(-d_{2m_1-1})$, and, by Lemma 16, there are exactly $\binom{2m_1-2}{m_1-2}$ distinct choices for $(d_1, \ldots, d_{2m_1-2}) \in \{\pm 1\}^{2m_1-2}$. In total, the number of possibilities for $(d_1, \ldots, d_{2m_1-2}) \in \{\pm 1\}^{2m_1-2}$ is

$$\binom{2m_1-2}{m_1-1} + \binom{2m_1-2}{m_1-2} = \binom{2m_1-1}{m_1-1} = \binom{2m_1-1}{m_1}.$$

Therefore, the total number of distinct choices of $\mathbf{d} \in \{\pm 1\}^n$ that satisfy (10) is

$$\binom{2m_1-1}{m_1}\binom{2m_2}{m_2}.$$

This number is also the number of facets of ∇_G whose facet subgraph is B, i.e.,

$$|\{F \in \mathcal{F}(\nabla_G) \mid G_F = B\}| = \binom{2m_1-1}{m_1}\binom{2m_2}{m_2}.$$

Recall that there are $2m_2$ corank-1 facet subgraphs. Therefore, the total number of corank-1 facets ∇_G has is

$$2m_2\binom{2m_1-1}{m_1}\binom{2m_2}{m_2}.$$

Combining the number of corank-0 and corank-1 facets, we can conclude that

$$|\,\mathcal{F}(\nabla_G)\,| = (2m_1-1)\binom{2m_1-2}{m_1-1}\binom{2m_2}{m_2} + 2m_2\binom{2m_1-1}{m_1}\binom{2m_2}{m_2},$$

which completes the proof. □

It has been shown that for a even cycle C_{2k}, the number of facets $\nabla_{C_{2k}}$ has is $\binom{2k}{k}$ [18]. Using this formula, we can relate the facet count presented above and the facet counts for adjacency polytopes associated with even cycles.

Corollary 18. *Let G be the graph formed by joining two cycles of size $2m_1$ and $2m_2+1$ respectively along a shared edge. Then*

$$|\mathcal{F}(\nabla_G)| = \frac{m_1 + 2m_2}{2} f_{C_{2m_1}} f_{C_{2m_2}},$$

where $f_{C_{2m_1}}$ and $f_{C_{2m_2}}$ are the number of facets $\nabla_{C_{2m_1}}$ and $\nabla_{C_{2m_1}}$ have respectively.

Acknowledgements

This project is motivated by a series questions posed by Tien-Yien Li in his 2013 lecture on solving polynomial systems. It is also an extension of a discussion the authors had with Alessio D'Alì, Emanuele Delucchi, and Mateusz Michałek.

References

[1] R. B. Bapat. *Graphs and Matrices.* Universitext. Springer, 2014.

[2] D. N. Bernshtein. The number of roots of a system of equations. *Functional Analysis and its Applications*, 9(3):183–185, 1975.

[3] T. Chen. Directed acyclic decomposition of Kuramoto equations. *Chaos: An Interdisciplinary Journal of Nonlinear Science*, 29(9):093101, sep 2019.

[4] T. Chen. Unmixing the Mixed Volume Computation. *Discrete and Computational Geometry*, mar 2019.

[5] T. Chen and R. Davis. A toric deformation method for solving Kuramoto equations. oct 2018. `http://arxiv.org/abs/1810.05690`.

[6] T. Chen, R. Davis, and D. Mehta. Counting Equilibria of the Kuramoto Model Using Birationally Invariant Intersection Index. *SIAM Journal on Applied Algebra and Geometry*, 2(4):489–507, jan 2018.

[7] T. Chen, J. Marecek, D. Mehta, and M. Niemerg. Three Formulations of the Kuramoto Model as a System of Polynomial Equations. mar 2016.

[8] T. Chen, D. Mehta, and M. Niemerg. A Network Topology Dependent Upper Bound on the Number of Equilibria of the Kuramoto Model. mar 2016.

[9] D. Cox. The homogeneous coordinate ring of a toric variety. *J Algebraic Geom.*, 4:17–50, 1995.

[10] A. D'Alì, E. Delucchi, and M. Michałek. Many faces of symmetric edge polytopes, 2019. `https://arxiv.org/abs/1910.05193`.

[11] E. Delucchi and L. Hoessly. Fundamental polytopes of metric trees via parallel connections of matroids. dec 2016. `http://arxiv.org/abs/1612.05534`.

[12] A. Higashitani, K. Jochemko, and M. Michałek. Arithmetic aspects of symmetric edge polytopes. *Mathematika*, 65(3):763–784, 2019.

[13] A. Higashitani, M. Kummer, and M. Michałek. Interlacing Ehrhart Polynomials of Reflexive Polytopes. dec 2016. `http://arxiv.org/abs/1612.07538`.

[14] B. Huber and B. Sturmfels. A polyhedral method for solving sparse polynomial systems. *Mathematics of Computation*, 64(212):1541–1555, 1995.

[15] Y. Kuramoto. Self-entrainment of a population of coupled non-linear oscillators. Lecture Notes in Physics, pages 420–422. Springer Berlin Heidelberg, 1975.

[16] T. Matsui, A. Higashitani, Y. Nagazawa, H. Ohsugi, and T. Hibi. Roots of Ehrhart polynomials arising from graphs. *Journal of Algebraic Combinatorics*, 34(4):721–749, dec 2011.

[17] H. Ohsugi and T. Hibi. Centrally symmetric configurations of integer matrices. *Nagoya Math. J.*, 216:153–170, 12 2014.

[18] H. Ohsugi and K. Shibata. Smooth fano polytopes whose ehrhart polynomial has a root with large real part. *Discrete and Computational Geometry*, 47(3):624–628, Apr 2012.

[19] F. Rodriguez-Villegas. On the zeros of certain polynomials. *Proceedings of the American Mathematical Society*, 130, feb 2002.

[20] A. Schrijver. *Theory of linear and integer programming.* John Wiley & Sons, 1998.

[21] G. M. Ziegler. *Lectures on polytopes.* Springer-Verlag, New York, 1995.